1 August 2002

Optics Communications 209 (2002) 181–192

OPTICS COMMUNICATIONS

www.elsevier.com/locate/optcom

Theoretical analysis of actively mode-locked fiber ring laser with semiconductor optical amplifier

Can Peng*, Minyu Yao, Janfeng Zhang, Hongming Zhang, Qianfan Xu, Yizhi Gao

Department of Electronic Engineering, University of Beijing, 100084 Beijing, China

Received 24 January 2002; received in revised form 4 April 2002; accepted 23 May 2002

Abstract

A theoretical study of active mode-locking fiber loop laser using semiconductor optical amplifier (SOA) was presented in this paper. The effects of linewidth broadening factor of SOA on active mode-locking were investigated originally. The relations between parameters of output pulse series and the critical parameters of SOA and other elements in fiber loop were obtained. © 2002 Elsevier Science B.V. All rights reserved.

Keywords: Theoretical model; Active mode-locking; Fiber laser; Semiconductor optical amplifier

1. Introduction

Ultra-short pulse sources are key devices for the future optical communications [1] and other all-optical data processing applications such as optical analog-digital (A/D) conversion [2] and optical logic devices [3]. Mode-locking lasers are preferable for generating ultra-short pulse series. Various mode-locked lasers with higher than 10 GHz repetition have been demonstrated [4–7]. A 40 GHz, 850 fs pulse series was obtained by using a mode-locking fiber loop laser with erbium-doped fiber as gain medium [4]. Recently semiconductor optical amplifier (SOA) was used as gain medium and modulator to generate 20 GHz, 4.3 ps pulse series by external optical modulation [5]. And 10 GHz, 3 ps pulse series was directly obtained from the actively mode-locked fiber ring laser with SOA and electro-absorption modulator (EAM) [6].

Our purpose in this paper is to present a general analytical model for operation of the actively mode-locked fiber ring laser with SOA and external amplitude modulator. There are some works investigating mode-locking laser theoretically [5,8–10,13]. These previous theories are not applicable to mode-locked lasers using SOA as gain medium. In [8] passive mode-locking laser using saturable absorber was analyzed in time-domain. A similar method was used in [9] to analyze active mode-locking laser. A method using the ABCD Law was presented in [10] to mode fiber ring laser using

* Corresponding author. Tel.: +01062772370; fax: +01062 770317.

E-mail address: pengcan00@mails.tsinghua.edu.cn (C. Peng).

PII: S0030-4018(02)01620-6

EDF. In [8–10] the gain variation in the pulse duration was not considered. However, the dynamic gain has to be considered to estimate the characteristics of the actively mode-locked fiber ring laser with a SOA.

In this paper a method was presented to model actively mode-locked fiber laser using a SOA, the variation of gain in the pulse duration was included and effects of self-phase modulation (SPM) in the SOA, which is induced by linewidth broadening factor of the SOA, were considered. The parameters of other components, which affect the laser performance, were also investigated. And some principles of active mode-locking laser designing are concluded.

The rest of this paper was organized as follows. In Section 2 the basic model was described and the time-domain method was introduced. The results were discussed in Section 3. Finally, conclusions were presented in Section 4.

2. Theoretical models

The configuration of actively mode-locked fiber ring laser is shown as Fig. 1, in which there is a SOA as gain medium in the ring and an amplitude modulator (AM) to modulate the loss in the cavity. The oscillating wavelength is chosen by a filter. Isolators make sure that light goes in one direction in the cavity. To obtain stable pulse series in the cavity, the modulating frequency of the modulator should be nearly integral times the fundamental frequency of the cavity, L_0/c (L_0 is the optical path, c is the velocity in vacuum). We assume that, in stable operation case, every pulse in the cavity has the same shape. The pulse shape is modified by the SOA, the filter and the modulator in the cavity; however, it is restored when the pulse comes back. The further assumptions are: (a) in the bandpass of filter, the gain variation in SOA with wavelength is negligible. (b) Chromatic dispersion in the cavity is negligible. (This will be dropped in Section 3.3.) (c) The bandpass of the filter is considered as a Gaussian shape near the band of pulses. In the following, models for components in the cavity are presented, and self-consistence equation is derived.

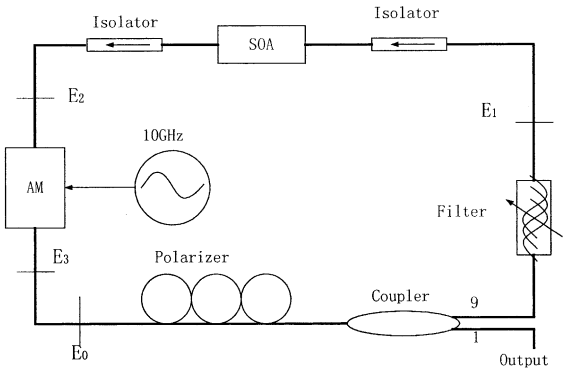

Fig. 1. Structure of fiber loop laser.

2.1. Semiconductor optical amplifier

The transfer function in time-domain of SOA is modeled as follows:

$$\hat{T}_{\mathrm{SOA}}(t) = \mathrm{e}^{G(t)(1+i\alpha)/2}, \tag{1}$$

where α is the linewidth broadening factor of the SOA [12] and $G(t)$ is the total power gain of SOA. It is given by

$$G(t) = \int_0^l g(z,t)\,\mathrm{d}z, \tag{2}$$

where $g(z,t)$ is local power gain at z and l is the length of SOA. The variation of $G(t)$ with time can be described by rate equation [14]

$$\frac{\mathrm{d}G(t)}{\mathrm{d}t} = \frac{G_{\mathrm{ss}} - G(t)}{\tau} - \frac{cn\varepsilon_0 A|E_{\mathrm{in}}(t)|^2}{2J_{\mathrm{sat}}}(\mathrm{e}^{G(t)} - 1), \tag{3}$$

where G_{ss} is the small signal gain of SOA, τ is the carriers' recovery time, A is the cross-section area of SOA, and J_{sat} is the saturation energy of SOA. And we define

$$J(t) = \frac{cn\varepsilon_0 A}{2}\int_{-\infty}^{t} |E_{\mathrm{in}}(t')|^2\,\mathrm{d}t'. \tag{4}$$

We neglect the recovery of carriers in pulse duration. So the solution of (3) is

$$1 - \mathrm{e}^{-G(t)} = (1 - \mathrm{e}^{-G_{\mathrm{in}}})\mathrm{e}^{-\frac{J(t)}{J_{\mathrm{sat}}}}. \tag{5}$$

In which G_{in} is the gain before the pulse coming in. Gain variation in pulse duration $G(t)$, which is

described accurately by (5), can be approximated by a linear function as

$$G(t) = \frac{G_{\text{in}} + G_{\text{out}}}{2} + \frac{G_{\text{out}} - G_{\text{in}}}{\sqrt{\pi}\Delta T} t. \tag{6}$$

The accuracy of this approximation is affected by the G_{in} and input pulse energy J_{total}, but when G_{in} is below 4.6 (about 20 dB) and input pulse energy is below $0.01J_{\text{sat}}$, which are satisfied in common cases, the error of this approximation is below 3% in the range of $2\Delta T$ near the pulse center. The G_{out} is the gain when the pulse goes out. And the relation between G_{in} and G_{out} is

$$1 - \mathrm{e}^{-G_{\text{out}}} = (1 - \mathrm{e}^{-G_{\text{in}}})\mathrm{e}^{-U_0}, \tag{7}$$

where $U_0 = J_{\text{total}}/J_{\text{sat}}$. And ΔT is determined by the shape of pulse, in Gaussian shape, it is the Gaussian pulsewidth. Out of the pulse duration, the gain recovery according to Eq. (3) without the second term on the right. In the stable state, the relation between the gain before the pulse coming in (G_{in}) and that after the pulse out (G_{out}) is

$$G_{\text{in}} = (G_{\text{out}} - G_{\text{ss}})\mathrm{e}^{-T_{\text{b}}/\tau} + G_{\text{ss}}, \tag{8}$$

where T_{b} is the recovery time between two pulses.

2.2. Amplitude modulator

The modulation characteristic of the AM is assumed as follows:

$$\hat{T}_{\text{mod}} = \exp\left[-\frac{L}{2} - \frac{\delta_{\text{m}}}{2}(1 - \cos\omega t)\right], \tag{9}$$

where L is the total static loss in the cavity at the central frequency of the filter, δ_{m} is the intensity of modulation, and ω is modulation frequency.

With the assumption that the pulsewidth of stable operation case is small compared with the modulation period, the cosine function can be expanded to the second term

$$\hat{T}_{\text{mod}}(t) = \exp\left[-\frac{L}{2} - \frac{\delta_{\text{m}}}{2}\omega^2 t^2\right]. \tag{10}$$

If the pulse passes through the modulator not at the peak of the transfer function, but shifted by a phase angle θ, the transfer function of modulator can be approximated by [9]

$$\begin{aligned}\hat{T}_{\text{mod}}(t) &= \exp\left[-\frac{L}{2} - \frac{\delta_{\text{m}}}{2}(1 - \cos(\omega t - \theta))\right] \\ &\cong \exp\left[-\frac{L}{2} - \frac{\delta_{\text{m}}}{2}(1 - \cos\theta) \right. \\ &\quad \left. + \frac{\delta_{\text{m}}}{2}\sin\theta\omega t - \frac{\delta_{\text{m}}}{4}\cos\theta\omega^2 t^2\right].\end{aligned} \tag{11}$$

When θ is positive, the pulse precedes to the peak of modulating signal, vice versa.

2.3. Filter

It is assumed that the filter has a Gaussian shape spectrum. So the frequency-domain transfer function is given by [9]

$$\hat{T}_{\text{filter}}(\omega) = \exp\left[-\frac{(\omega - \delta\omega)^2}{2\Delta\omega_{\text{g}}^2}\right], \tag{12}$$

where $\Delta\omega_{\text{g}}$ has a relation with the full width at half maximum (FWHM) of the transfer spectrum of the filter as follows:

$$\Delta\omega_{\text{g}} = \frac{1}{2\sqrt{\ln 2}}\Delta\omega_{\text{FWHM}}. \tag{13}$$

It is assumed that there is a frequency shift as much as $\delta\omega$ between the central frequency of pulse and that of the filter. $\delta\omega$ is not zero due to SPM in SOA.

2.4. Pulse shape

In this model, the pulse is assumed to be Gaussian pulse instead of sech pulse in [5,8]. The electric field is presented by

$$E_0(t) = \left(\frac{U_0 J_{\text{sat}}}{\sqrt{\pi}\Delta T}\right)^{1/2} \mathrm{e}^{-\frac{(1+\mathrm{i}\beta)t^2}{2\Delta T^2}}, \tag{14}$$

where $\Delta T = \Delta T_{\text{FWHM}}/(2\sqrt{2})$, and β is the linear chirp. Then substituting (14) into (4), it is obtained that

$$\begin{aligned}\frac{J(t)}{J_{\text{sat}}} &= \frac{nc\varepsilon_0 A}{2}\frac{\int_{-\infty}^{t}\mathrm{e}^{-\frac{t'^2}{\Delta T^2}}\mathrm{d}t'}{J_{\text{sat}}}, \\ U_0 &= \frac{J_{\text{total}}}{J_{\text{sat}}} = \frac{nc\varepsilon_0 A\Delta T\sqrt{\pi}}{2}\frac{1}{J_{\text{sat}}}.\end{aligned} \tag{15}$$

2.5. Self-consistence equation

With the models of the components in the loop laser presented above, the self-consistence equation of stable mode-locked pulse can be obtained. In the following, t is the retard frame time.

$$E_1(\omega) = \hat{T}_{\text{filter}}(\omega)E_0(\omega). \tag{16}$$

After Fourier transformation

$$E_1(t) = \left(\frac{U_0 J_{\text{sat}}}{\sqrt{\pi}\Delta T}\right)^{1/2} \mathrm{e}^{\eta + \mathrm{i}\xi}\,\mathrm{e}^{-\gamma(t-T_{\text{d1}})^2}, \tag{17}$$

where

$$\frac{1}{\gamma} = \frac{2\Delta T^2}{1+\mathrm{i}\beta} + \frac{2}{\Delta\omega_{\text{g}}^2}, \quad T_{\text{d1}} = -\frac{\delta\omega}{\Delta\omega_{\text{g}}^2}\frac{\text{Im}(\gamma)}{\text{Re}(\gamma)}. \tag{18}$$

After pulse goes through the SOA,

$$\begin{aligned} E_2(t) &= \hat{T}_{\text{SOA}}(t - T_{\text{d1}})E_1(t) \\ &= \left(\frac{U_0 J_{\text{sat}}}{\sqrt{\pi}\Delta T}\right)^{1/2} \mathrm{e}^{\eta_1 + \mathrm{i}\xi_1}\,\mathrm{e}^{-\gamma(t-T_{\text{d2}})^2}. \end{aligned} \tag{19}$$

With the same manner, the pulse out from modulator is

$$E_3(t) = \hat{T}_{\text{mod}}(t - T_{\text{d2}})E_2(t). \tag{20}$$

Including detuning between the modulating frequency and harmonic frequency of the cavity, there is

$$\frac{L_{\text{o}}}{c} = nT_{\text{m}} - \delta T, \tag{21}$$

where L_{o} is length of optical path of the cavity, T_{m} is the modulating period, and n is a integral. Then in stable operation case, there is

$$E_0(t - \delta T)\,\mathrm{e}^{\mathrm{i}\phi} = E_3(t), \tag{22}$$

where ϕ is a constant phase delay. This is the self-consistence equation.

2.6. Solution of self-consistence equation

Substituting equations into (22), and after some tedious derivation, a set of nonlinear equations is obtained

$$\text{Re}(\gamma) + \frac{\delta_{\text{m}}}{4}\omega_{\text{m}}^2\cos\theta - \frac{1}{2\Delta T^2} = 0, \tag{23.1}$$

$$\text{Im}(\gamma) - \frac{\beta}{2\Delta T^2} = 0, \tag{23.2}$$

$$\frac{G_{\text{in}} - G_{\text{out}}}{2\sqrt{\pi}\Delta T}\alpha - 2\frac{\delta\omega}{\Delta\omega_{\text{g}}^2}\text{Re}(\gamma) = 0, \tag{23.3}$$

$$\begin{aligned} &2\frac{\delta\omega}{\Delta\omega_{\text{g}}^2}\text{Im}(\gamma) - \frac{G_{\text{out}} - G_{\text{in}}}{2\sqrt{\pi}\Delta T} - \frac{\delta_{\text{m}}}{2}\omega_{\text{m}}^2\cos\theta T_{\text{d2}} \\ &\quad - \frac{\delta_{\text{m}}}{2}\omega_{\text{m}}\sin\theta + \frac{\delta T}{\Delta T^2} = 0, \end{aligned} \tag{23.4}$$

$$\begin{aligned} &\frac{G_{\text{in}} + G_{\text{out}}}{4} + \eta_1 - \frac{\delta_{\text{m}}}{2}(1 - \cos\theta) - \frac{\delta_{\text{m}}}{2}\omega_{\text{m}}\sin\theta T_{\text{d2}} \\ &\quad - \frac{\delta_{\text{m}}}{4}\omega_{\text{m}}^2\cos\theta T_{\text{d2}}^2 - \frac{G_{\text{out}} - G_{\text{in}}}{2\sqrt{\pi}\Delta T}T_{\text{d1}} \\ &\quad - \frac{L}{2} + \frac{\delta T^2}{2\Delta T^2} = 0, \end{aligned} \tag{23.5}$$

with Eqs. (7) and (8) where $T_{\text{b}} = 2\pi/\omega - \sqrt{\pi}\Delta T/2$, there are seven equations and seven unknowns, $\Delta T, \beta, G_{\text{in}}, G_{\text{out}}, U_0, \delta\omega$ and θ. These equations can be solved by using the tools in matlab, which is based on least squares algorithm.

With (23.2) and (18), it can be derived that the linear chirp at the pulse center, β, is zero. From (23.1) and with an assumption that the spectrum width of the pulse is much smaller than the pass bandwidth of the filter, it can be obtained

$$\Delta T \simeq \sqrt[4]{\frac{2}{\Delta\omega_{\text{g}}^2\omega_{\text{m}}^2\delta_{\text{m}}\cos\theta}}. \tag{24}$$

It is noteworthy that because of the linewidth broadening factor α of SOAs, there is Eq. (23.3), which was not included in previous publications. The leaded frequency shift $\delta\omega$ affects the loss in the cavity and then affects the pulse power and pulsewidth. It is included implicitly in η_1 in (23.5). From (23.3), the frequency shift from the center frequency of the filter can be obtained

$$\delta\omega = \frac{(G_{\text{in}} - G_{\text{out}})\Delta\omega_{\text{g}}^2}{4\sqrt{\pi}\Delta T\text{Re}(\gamma)}\alpha. \tag{25}$$

Because α is positive, $\delta\omega$ is also positive. The center frequency of the pulse shifts to lower frequency (long wavelength) from the center frequency of the filter, this can be shown in the spectrum in [6].

From (23.1)–(23.5), let $U_0 = 0$, the minimum G_{ss} is obtained

$$G_{\mathrm{ss}_{\min}}(\mathrm{dB}) = L(\mathrm{dB}) + \frac{10}{\ln 10}\sqrt{\frac{\omega_{\mathrm{m}}^2\delta_{\mathrm{m}}}{\Delta\omega_{\mathrm{g}}^2}}. \quad (26)$$

Below this threshold the power of the pulse in stable operation case is zero.

3. Results and discussion

In this section, the performances of fiber ring laser with SOA were investigated. The effects of some critical parameters on the performance were estimated.

3.1. Pulsewidth and peak power

The pulsewidth in stable operation case can be expressed as (24). It shows that the pulsewidth is determined by filter bandwidth, $\Delta\omega_{\mathrm{g}}$, modulation intensity, δ_{m}, the phase shift between pulse train and modulating signal, θ, and the modulating frequency ω_{m}. In the following discussion ω_{m} is assumed to be 10 GHz. And the saturated energy of the SOA is assumed to be 5 pJ.

Fig. 2 shows the effect of modulation intensity on the pulsewidth and peak power of the stable output pulses. Larger modulation intensity leads to shorter pulsewidth and larger peak power. When δ_{m}, varies from 1 to 5, the pulsewidth reduces more than 3.5 ps and the peak power doubles. The effect of bandwidth of filter is depicted in Fig. 3. It seems that large bandwidth filter is preferable. The broader the filter is, the shorter the output pulses and the higher the peak power. From (24), it can be learned that the pulsewidth is also influenced by θ. This variant is relevant to many parameters of the ring laser. So other parameters also have effects on the output pulsewidth and the peak power.

Fig. 4 reports the effects of small signal gain. Large small signal gain will broaden the pulsewidth, but this effect is not remarkable. However small signal gain has important influence on the peak power of the pulses. At first, large small signal gain leads to nonuniformity of pulse power

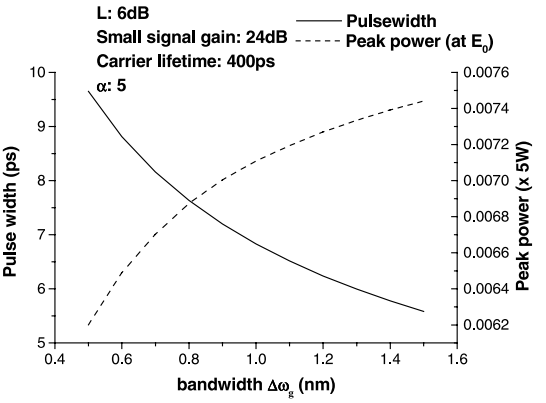

Fig. 3. Effects of the bandwidth of the filter on the pulsewidth and peak power of the output pulses.

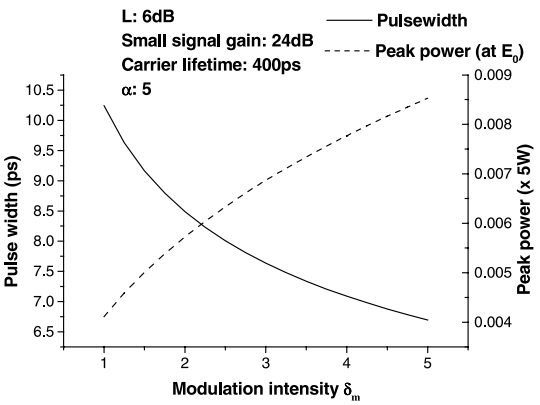

Fig. 2. Effects of modulation intensity on the pulsewidth and peak power of the output pulses.

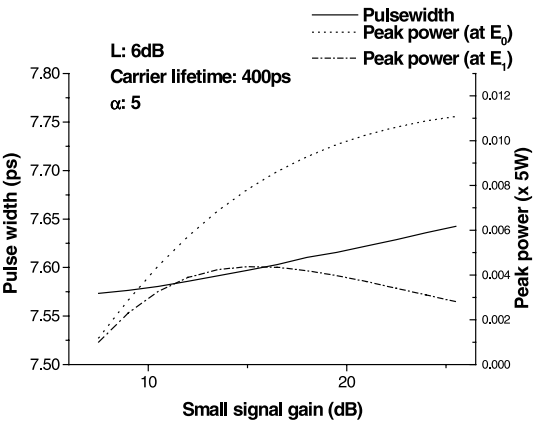

Fig. 4. Effects of small signal gain on the pulsewidth and peak power of the output pulses.

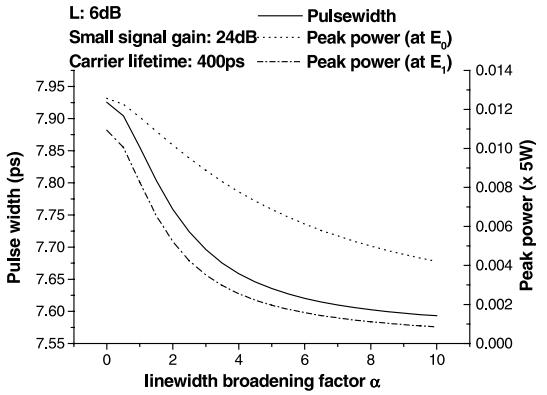

Fig. 5. Effects of linewidth broadening factor on the pulsewidth and peak power of the output pulses.

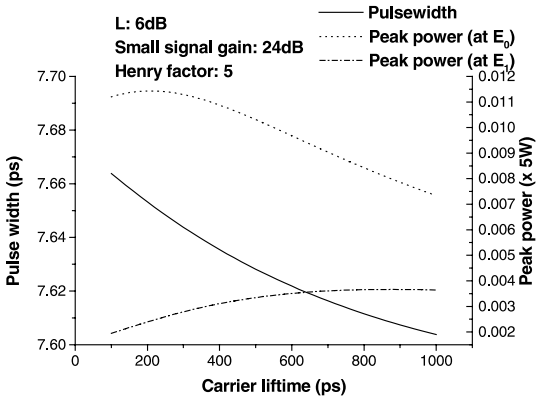

Fig. 6. Effects of carrier lifetime on the pulsewidth and peak power of the output pulses.

in cavity. Fig. 4 shows peak powers at two different positions, at E_0 and E_1 referred to Fig. 1. The output peak power at E_0 increases as the small signal gain increases, but the peak power at E_1 (or input port of SOA) decreases when small signal gain is too large. This is because large small signal gain leads to large gain variation during the pulse, which leads to large frequency shift from the transmission peak of the filter, then the loss in the filter increases, and the input pulses of the SOA become weak.

The linewidth broadening factor of SOA, α, also has effects on the pulsewidth and peak power. It is depicted in Fig. 5. The variation of pulsewidth is not very remarkable, however, the peak power decreases rapidly. It means that SOA with small α is helpful to achieve large output power.

The effects of carrier lifetime of SOA are reported in Fig. 6. Pulses will become shorter when lifetime increases, the peak power of pulses decreases as well. And from the difference between the peak power before and after SOA, it can be found that the shorter the carrier lifetime, the larger the average gain of SOA during the pulse passing by.

Another parameter of the ring laser, which has effects on the peak power, is the static loss in cavity. It can be obtained that less static loss in cavity leads to higher peak power in Fig. 7. Fig. 7(a) shows the relation between the peak power at the input port of SOA (at E_1) and difference

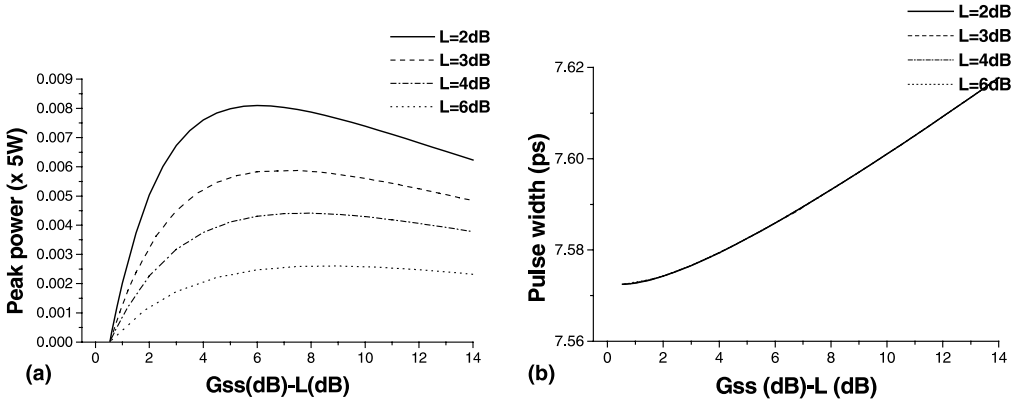

Fig. 7. Effects of static cavity loss on the pulsewidth and peak power of the output pulses.

between small signal gain and static cavity loss. From Fig. 7(b), we find that the curves of pulsewidth versus difference between small signal gain and static cavity loss overlap for different static cavity loss. So the pulsewidth is irrelevant to static cavity loss, but the difference between small signal gain and cavity loss has effects on the pulsewidth.

From Fig. 7(a) the threshold small signal gain also can be seen. And when the small signal gain approaches the threshold, the pulsewidth approaches the lower limitation of pulsewidth which is set by modulation intensity, bandwidth of filter and modulating frequency

$$\Delta T_{\mathrm{FWHM}_{\min}} = 2\sqrt{\ln 2}\sqrt[4]{\frac{2}{\Delta\omega_{\mathrm{g}}^2\omega_{\mathrm{m}}^2\delta_{\mathrm{m}}}}. \tag{27}$$

It also shows that there is an optimistic small signal gain to obtain largest peak power at the input port of SOA and to get smallest noise figure [11]. This optimistic G_{ss} is larger than static cavity loss by about 6 dB.

3.2. Frequency shift and phase leading of the pulses

In this section, the frequency shift of the pulses due to SPM in SOA and the phase leading of the pulses to the modulating signal are presented.

When pulses go through the SOA, the index of this device varies in time as well as the gain due to the depletion of carriers. Near the center of the pulse, the variation of the phase is approximately linear and with negative slope in time, so there should be a red shift when pulses pass through the SOA. In the stable operation case, the pulse field should be restored after a round trip, and then the red shift of frequency induced by SPM in SOA is compensated partly in the filter. Therefore the center of pulses spectrum must be at the positive slope side (in frequency domain) of the spectrum of the filter, the positive slope side can compensate the red shift by reducing the low frequency component in pulses. So there is a frequency shift between the center frequency of pulses and the filter. Maybe it is related to the stability in the fiber ring laser with SOA, because the high power pulse will get large red shift and then suffer large loss in the filter. The fluctuation in the pulse train is therefore suppressed.

Due to the variation of gain in the pulse duration, the pulse shape is modified and the location of pulse peak changes in time. To restore these changes, pulses cannot pass the modulator at the peak of modulating signal, but have some phase leading.

Fig. 8 shows the effects of linewidth broadening factor on the frequency shift and phase leading. The red shift of pulse frequency from the center frequency of the filter increases as the linewidth broadening factor increases. But the increasing rate decreases because of the reduction of pulse power. From (24), it can be seen that the phase leading θ is relevant to the pulsewidth. Increasing phase leading leads to decrease of $\cos\theta$, and then increase of the pulsewidth. Fig. 8 shows that $\cos\theta$ increases with the increase of α, and the pulsewidth decreases, which is consistent to the result in Section 3.1.

The effects of small signal gain on the frequency shift and phase leading are depicted in Fig. 9. Large small signal gain will lead to large red shift in frequency, because the larger the small signal gain is, the larger the variation of the gain and the index of the SOA. We can see $\cos\theta$ decrease when small signal gain becomes large from Fig. 9. Then the pulsewidth is broadened when small signal gain increase. This also verifies that reported by Fig. 4.

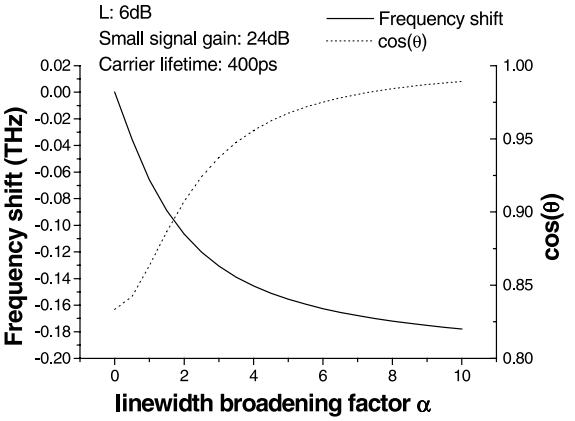

Fig. 8. Effects of linewidth broadening factor on the frequency shift and phase leading of pulses.

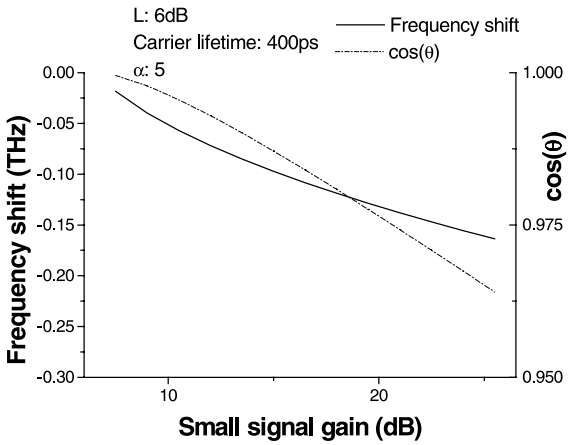

Fig. 9. Effects of small signal gain on the frequency shift and phase leading of pulses.

Carrier lifetime also has effects on the frequency shift and phase leading. Long carrier lifetime will lead to small difference between G_{in} and G_{out}, then the variation of carrier density in pulse duration is small. So the red shift is small when carrier lifetime is long as shown in Fig. 10. Small variation of gain in pulse duration also leads to small phase leading of pulses to modulating signal. The variation of $\cos\theta$ with that of carrier lifetime is also reported in Fig. 1, and the pulsewidth variation leaded by that is consistent to the result obtained in Section 3.1.

That the frequency red shift decreases with the increase of the modulation intensity is shown in

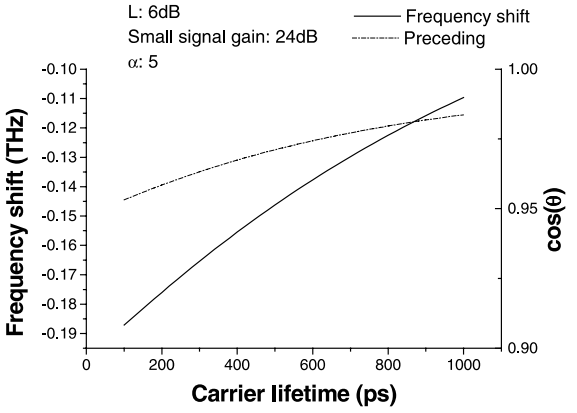

Fig. 10. Effects of carrier lifetime on the frequency shift and phase leading of pulses.

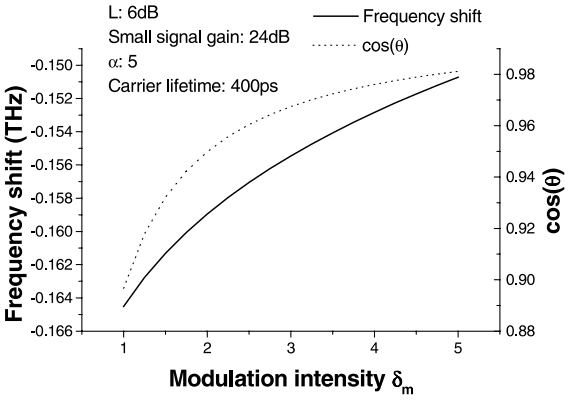

Fig. 11. Effects of modulation intensity on the frequency shift and phase leading of pulses.

Fig. 11. This is because large modulation intensity leads to small average gain during pulse due to large pulse power, and then small variation of gain during pulse, which finally leads to small frequency red shift. Fig. 11 also shows that $\cos\theta$ increases with the increase of modulation intensity, and the variation of the pulsewidth is just as reported in Fig. 2.

The modulation frequency ω_m and filter bandwidth ω_g have effects on the pulsewidth as shown in (27). But numerical analysis shows that they have no significant effect on phase leading θ.

In all factors that affect θ, the modulation intensity is easy to vary and its effects is more significant, so it affects the value of θ most.

3.3. Dispersion and chirp

From (23.1)–(23.5) we can find that when the dispersion in the cavity is zero, the chirp parameter β is zero too. But when there is nonzero total group velocity dispersion (GVD), D (ps^2), the output pulses will have chirp. The transfer function of dispersion is

$$\hat{T}_{disp} = \exp\left(\frac{i}{2}D\omega^2\right). \tag{28}$$

Add this term into the self-consistent equation, and we will get a more complicated set of equations than (23.1)–(23.5). The effects of total GVD D on the pulse chirp parameter β and pulsewidth are depicted in Fig. 12.

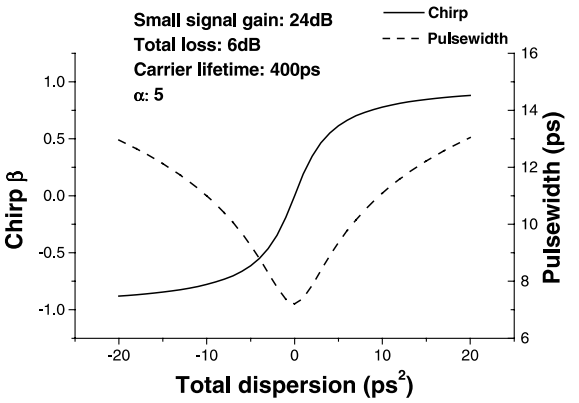

Fig. 12. Effects of dispersion on chirp parameter and pulsewidth.

Large total GVD will lead large chirp and large pulsewidth. It is noteworthy that we use $e^{i\omega t}$ system in this paper, so positive β stands for negative chirp. In the SOA ring laser the cavity length is about 20 m and it is composed of single mode fiber (SMF), so the total GVD is about 0.4 ps^2. For the short cavity length, pulse chirp is negligible for the SOA ring laser.

Numerical analysis also shows that the linewidth broadening factor α has little effect on the chirp parameter β, but it leads the frequency shift of the pulse central frequency from the transmission peak of filter as shown in Section 3.2.

3.4. Stability range

Because there is ASE noise in SOA, the net gain in the cavity before the pulse comes in and that after the pulse goes out should be negative to suppress noise at both edges [13]. Then there is

$$\begin{aligned} &G_{\text{in}} - L - \delta_{\text{m}}\cos\theta - \frac{\delta_{\text{m}}}{2}\sqrt{\pi}\omega\sin\theta\Delta T \\ &\quad - \frac{\delta_{\text{m}}}{8}\pi\omega^2\cos\theta\Delta T^2 < 0, \\ &G_{\text{out}} - L - \delta_{\text{m}}\cos\theta - \frac{\delta_{\text{m}}}{2}\sqrt{\pi}\omega\sin\theta\Delta T \\ &\quad - \frac{\delta_{\text{m}}}{8}\pi\omega^2\cos\theta\Delta T^2 < 0. \end{aligned} \tag{29}$$

Equations (29) together with (26) specify a stability range of small signal gain of the SOA to get stable operation of the ring laser. Numeric solution of the equations shows that the lower limitation of the stability range is the threshold specified by (26), the range between the upper limitation and the lower limitation is determined by linewidth broadening factor, carrier lifetime, bandwidth of filter and modulation intensity but irrelevant to the cavity loss.

Fig. 13 shows the effects of carrier lifetime on the size of stability range. The size of stability range increases almost linearly with the increase of carrier lifetime.

The linewidth broadening factor also has effects on the size of stability range. It is shown in Fig. 14. The size of stability range is small under large linewidth broadening factor. It is reason-

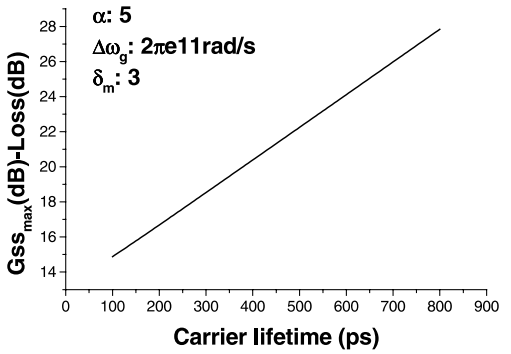

Fig. 13. The effects of carrier lifetime on the size on the stability range.

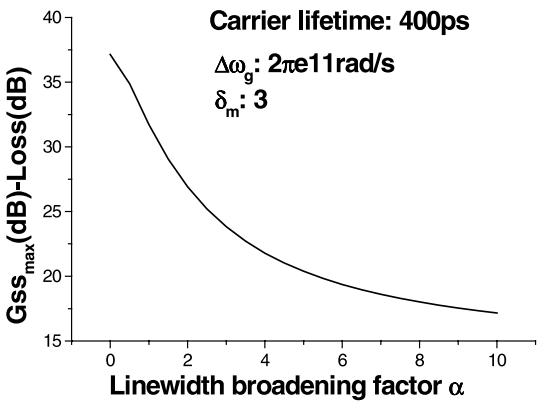

Fig. 14. The effects of linewidth broadening factor of stability range.

able. Because large α leads to large red shift in frequency of pulses, the pulses suffer large loss in the filter, while the loss that noise suffers does not increase, for its broad spectrum. Then the conditions of stability are tended to be broken.

Large modulation intensity leads to large stability range is shown in Fig. 15. And the size of stability range decreases while the bandwidth of the filter increases, but it is not very significant. It also should be noted that under different modulation intensity and bandwidth, the threshold of small signal is different, but fortunately the difference is negligible.

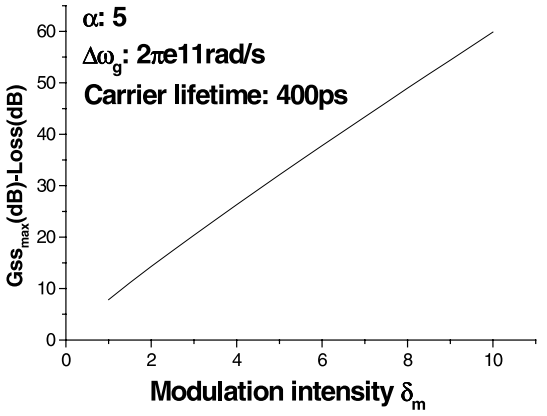

Fig. 15. The effects of modulation intensity on the size of stability range.

3.5. Effects of detuning

This subsection considers there is a detuning between the fundamental frequency and the modulating frequency. That is to say δT in (21) is not zero. δT can be in $(-50, 50]$ ps when the modulating frequency is 10 GHz. The following picture shows the effects of detuning on the performance of the laser (see Fig. 16).

As is expected, the pulsewidth broadens rapidly and the peak power drops down dramatically when the detuning grows up. The shift of pulse central frequency from the central frequency of the filter reduces at first and then increase rapidly when detuning grows up. The preceding or delay of the pulse to the modulating signal increases as the detuning increases. It approaches 25 ps or $\pi/2$ in phase when detuning approaches half fundamental frequency.

When the detuning is too big and the pulsewidth is too large to assume that the carriers do not recover in pulse duration, the accuracy of this model decreases.

4. Conclusion

A self-consistence method was modified to model an active mode-locked fiber ring laser that uses a SOA as the gain material. The self-phase modulation of stable mode-locked pulses was

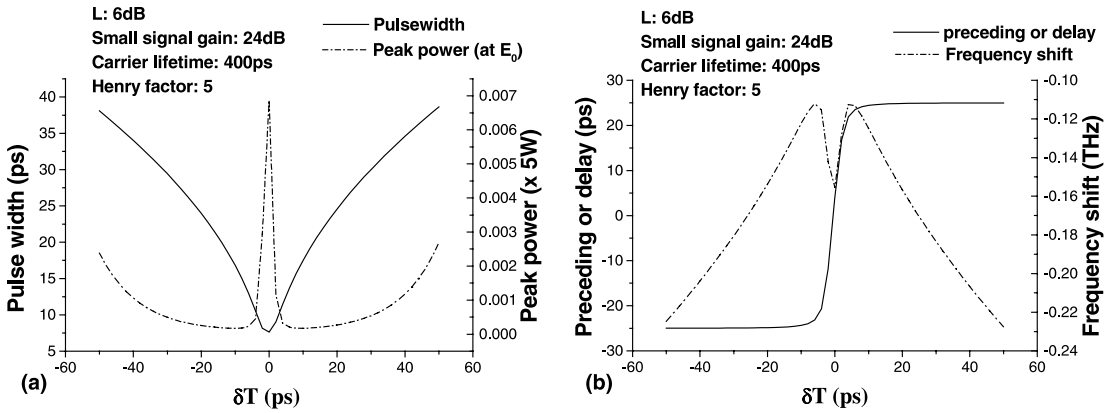

Fig. 16. (a) Effects of detuning on the pulsewidth and the pulse peak power. (b) Effects of detuning on frequency shift of the pulse and phase leading of the pulse to the modulating signal.

included. The effects of parameters of the SOA and other elements were investigated thoroughly.

As a gain material, SOAs have a characteristic – the variation of the reflectivity index with that of the gain caused by the linewidth broadening factor, which is different from some other gain materials, for example, erbium-doped fiber (EDF). These effects had been included originally, which were never considered in active mode-locking lasers before as we known. Positive linewidth broadening factor will not lead to linear chirp in the central of mode-locking pulse if the chromatic dispersion is negligible, but lead to the shift of central frequency of mode-locking pulse from that of the filter. This is because the gain variation during the pulse is approximately linear to time, but not parabolic. Linear gain variation integrated with linewidth broadening factor leads to frequency shift, but no chirp. Of course linewidth broadening factor causes chirp at both edges of the pulse, this cannot be investigated by this mode. The linewidth broadening factor also has effects on the pulsewidth and the peak power. A large linewidth broadening factor leads to small pulsewidths and small peak power at the same time. In addition large linewidth broadening factor narrows the stability range of small signal gain.

There is a threshold of the small signal gain of the SOA to get mode-locked pulses. And the net gain before and after a pulse should be negative in order to suppress noise, so there are extra boundaries of small signal gain. Calculations show that puts an upper limitation on the small signal gain. Between the threshold and the upper limitation is the stability range of small signal gain.

Large small signal gain will lead to broad mode-locked pulses in stability state and big noise, but too low small signal gain will lead to low peak power of the pulse. Then there is tradeoff to choose a proper small signal gain.

The total dispersion in the cavity leads the chirp in pulses and broadens the pulsewidth. Abnormal dispersion leads to positive chirp, and vice versa. Unlike the direct modulation of the SOA, linewidth broadening factor has little effect on the pulse chirp. And fortunately, the SOA ring is short (about 20 m), and the total dispersion is negligible. So the chirp and pulse broadening is not significant.

Long carrier lifetime of the SOA is preferable to get short pulse and larger stability range of small signal gain, but it also suppresses the power of the pulse in stable operation case.

The less the cavity loss, the larger the power at certain small signal gain. So the loss of the cavity should be reduced as much as possible. Of cause, the small signal gain of the SOA should be reduced to a proper value as well.

The modulation intensity and the bandwidth of the filter set the lower limitation of the pulsewidth. Large modulation intensity and large bandwidth filter lead to decrease of the pulsewidth limitation. But the modulation intensity is limited by the modulator's parameters. And large bandwidth filter will brings up the noise and narrows stability range of small signal gain.

The parameters just as pulsewidth, peak power, frequency shift and so on are also investigated when there is a detuning between modulating frequency and the fundamental frequency of the cavity.

Acknowledgements

This work is supported by Natural Science Foundation Committee of China (NSFC No. 60077001) and the foundation of Education Ministry.

References

[1] K. Emura, in: OSA Trends in Optics and photonics (TOPS), vol. 54, Optical Fiber Communication Conference, Technical Digest, Postconference, Optical Society of America, Washington, DC, 2001, Edition ML1-1.
[2] R.C. Thomas Jr., in: OSA Trends in Optics and photonics (TOPS), vol. 54, Optical Fiber Communication Conference, Technical Digest, Postconference, Optical Society of America, Washington, DC, 2001, Edition WV1-1.
[3] T.C. She, C. Shu, Electron. Lett. 30 (1) (1994) 81.
[4] M. Nakazawa, E. Yoshida, IEEE Photon. Tech. Lett. 12 (12) (2000) 1613.
[5] K. Zoiros, T. Stathopoulos, et al., Opt. Commun. 180 (2000) 301.

[6] M.J. Guy, J.R. Taylor, et al., Electron. Lett. 32 (24) (1996) 2240.
[7] D.H. Kim, S.H. Kim, et al., Opt. Commun. 181 (2000) 385.
[8] H.A. Haus, J. Appl. Phys. 46 (7) (1975) 3049.
[9] D.J. Kuizenga, A.E. Siegman, IEEE J. Quantum Electron. QE-6 (11) (1970) 694.
[10] Y. Li, C. Lou, et al., IEEE Photon. Tech. Lett. 11 (12) (1999) 1590.
[11] G. Giuliani, D. D'Alessandro, J. Lightwave Tech. 18 (9) (2000) 1256.
[12] C.H. Henry, IEEE J. Quantum Electron. QE-19 (9) (1983) 1931.
[13] R.G.M.P. Koumans, R. van Roijen, IEEE J. Quantum Electron. 32 (3) (1996) 478.
[14] G.P. Agrawal, N.A. Olsson, IEEE J. Quantum Electron. 25 (11) (1989) 2297.